Ice Prediction Workshop 2
Test Case Descriptions

IPW Organizing Committee

September 29, 2023

Revision log

- October 25, 2022
  - Initial version
- February 7, 2023
  - IRT cloud calibration data added for CRM65 cases simulation parameters
  - RG-15 AoAs changed to 4-degrees
  - RG-15 span changed from 590 to 580 mm
  - List of references
- February 23, 2023
  - Added IRT drop size distribution
  - Added recommended attachment line locations for CRM65 cases
- March 21, 2023
  - Added RG-15 droplet size distribution
  - Corrected the 1-bin droplet size for the RG-15 cases from 24 microns to 23 microns.
- March 22, 2023
  - Effect of the ceiling gap in the CRM65 cases
- April 28
  - Corrected the remarks on CAD and grids for the CRM65 cases: CADs provided at 0°, rotated +3.7° in Y axis about 0, 0, 0 to build the grids
- September 29
  - Defined location of static pressure used to calculate experimental Cp values for Cases1 and 2 (slide 12)
  - Defined uncertainty in aerodynamic and icing conditions for Cases 1 and 2 (slide 12)
  - Updated Case 3 conditions

Configurations Summary

Case 1: CRM-65 Mid-span Hybrid (3D)

Case 2: CRM-65 Inboard Hybrid (3D)

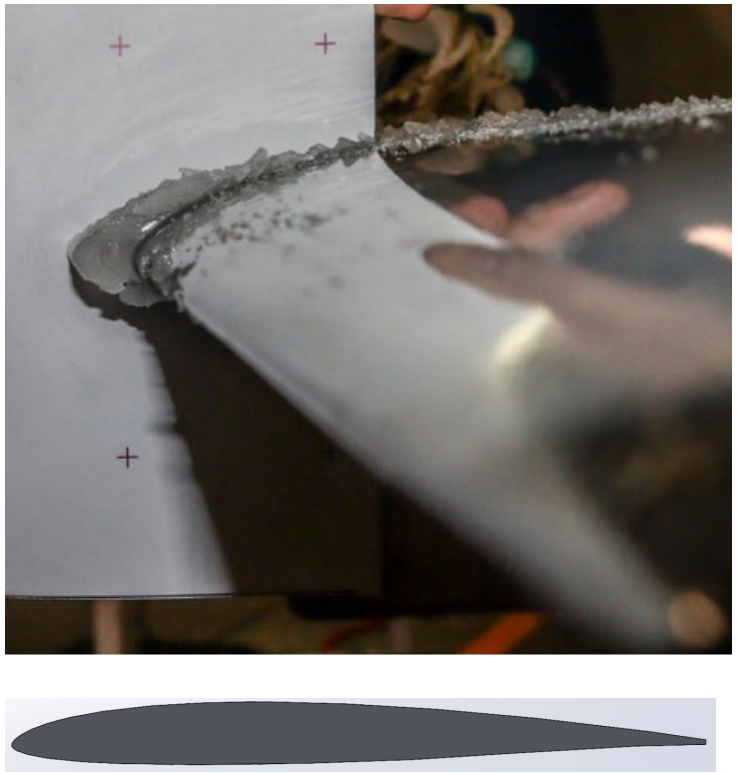

Case 3: RG-15 Low Speed Icing

Case list overview

IPW-2 Case no.	Configuration	AoA	Speed	T_{static} (°C)	T_{total} (°C)	LWC (g/m^3)	MVD (µm)	Icing Time (minutes)
1.1	CRM65 Mid-span	3.7	130 kts	-3.6	-1.4	1.0	25	29
1.2	CRM65 Mid-span	3.7	130 kts	-8.5	-6.3	1.0	25	29
1.3	CRM65 Mid-span	3.7	130 kts	-26.0	-23.8	1.0	25	29
2.1	CRM65 Inboard	3.7	130 kts	-3.6	-1.4	1.0	25	29
2.2	CRM65 Inboard	3.7	130 kts	-8.5	-6.3	1.0	25	29
2.3	CRM65 Inboard	3.7	130 kts	-26.0	-23.8	1.0	25	29
3.1	RG-15 Small wing	4	25 m/s	-2.0	-1.7	0.52*	27*	20
3.2	RG-15 Small wing	4	25 m/s	-4.0	-3.7	0.52*	27*	20
3.3	RG-15 Small wing	4	25 m/s	-10.0	-9.7	0.52*	27*	20

*Note, these values were updated after IPW2.

Cases 1.1-1.3: CRM65 Midspan

IPW-2 Case no	AoA (deg.)	Flap angle (deg.)	Speed (knots)	Speed (m/s)	T_{total} (°C)	T_{static} (°C)	P_{total} (kPa)	P_{static} (kPa)	MVD (μm)	LWC (g/m^3)	Time (min.)	Freezing fraction	2015 ice mass (kg/m)	2021 ice mass (kg/m)	2022 ice mass (kg/m)
1.1	3.7	25.0	130	66.9	-1.4	-3.6	99.3	96.5	25	1.0	29.0	0.12	4.17	3.75	3.70
1.2	3.7	25.0	130	66.9	-6.3	-8.5	97.5	94.7	25	1.0	29.0	0.35	6.42	6.64	5.93
1.3	3.7	25.0	130	66.9	-23.8	-26.0	99.3	96.3	25	1.0	29.0	1.00	6.5	5.43	5.30

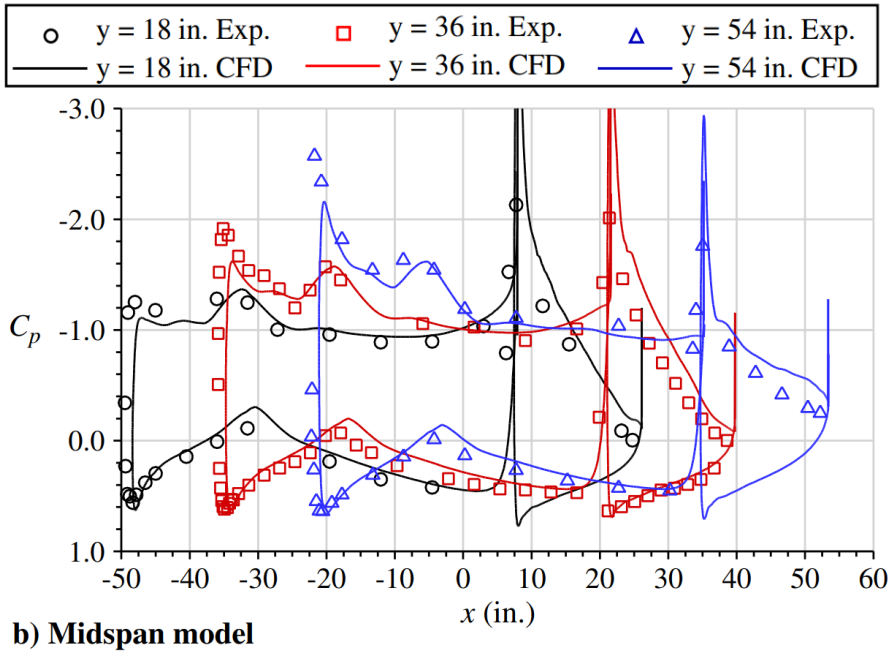

b) Midspan model

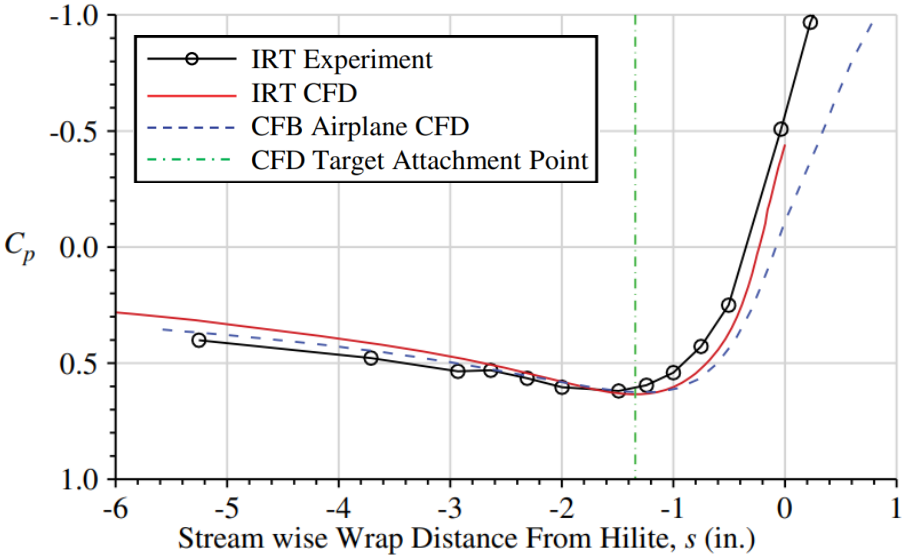

b) Midspan model

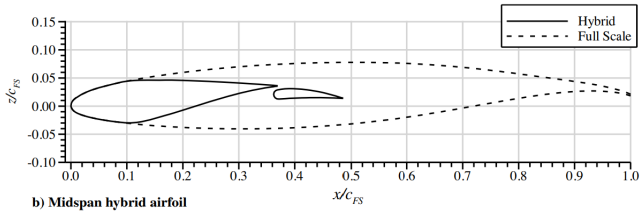

b) Midspan hybrid airfoil

- Workshop CADs provided at α = 0°, with the flap deflection built-in
- Grids are built after rotating the main element & flap assembly by +3.7° in Y axis about 0, 0, 0
- Pressure coefficients are based on inlet static pressure and density: CFD results that set back pressure at tunnel exit should use converged inlet static pressure as reference when computing C_P.

References: *Broeren et al., "*Ice-Accretion Test Results for Three Large-Scale Swept-Wing Models in the NASA Icing Research Tunnel", AIAA Aviation Forum, AIAA 2016-3733
Fujiwara, Bragg, Broeren, "Comparison of Computational and Experimental Ice Accretions of Large Swept Wings", J of A, Vol 57, No 2, 2020

Cases 1.1-1.3: CRM65 Mid-span: Comparison of MCCS

IPW-2 Case no	AoA (deg.)	Flap angle (deg.)	Speed (knots)	Speed (m/s)	T_{total} (°C)	T_{static} (°C)	P_{total} (kPa)	P_{static} (kPa)	MVD (μm)	LWC (g/m^3)	Time (min.)	Freezing fraction	2015 ice mass (kg/m)	2021 ice mass (kg/m)	2022 ice mass (kg/m)
1.1	3.7	25.0	130	66.9	-1.4	-3.6	99.3	96.5	25	1.0	29.0	0.12	4.17	3.75	3.70
1.2	3.7	25.0	130	66.9	-6.3	-8.5	97.5	94.7	25	1.0	29.0	0.35	6.42	6.64	5.93
1.3	3.7	25.0	130	66.9	-23.8	-26.0	99.3	96.3	25	1.0	29.0	1.00	6.5	5.43	5.30

Test Condition 2

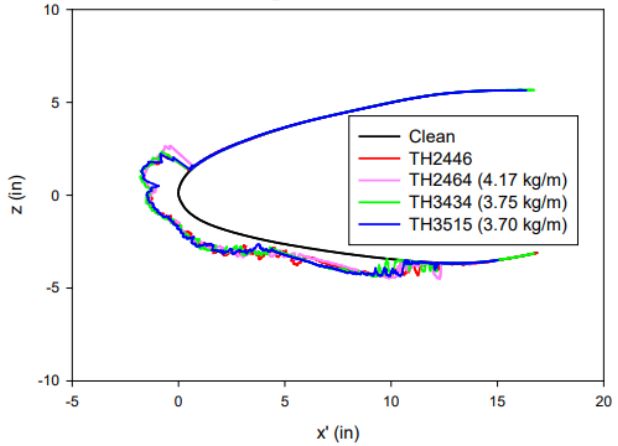

Case 1.1

Test Condition 4

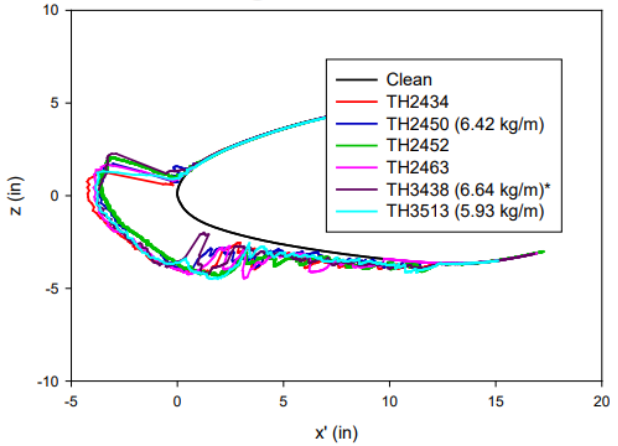

Case 1.2

Test Condition 8

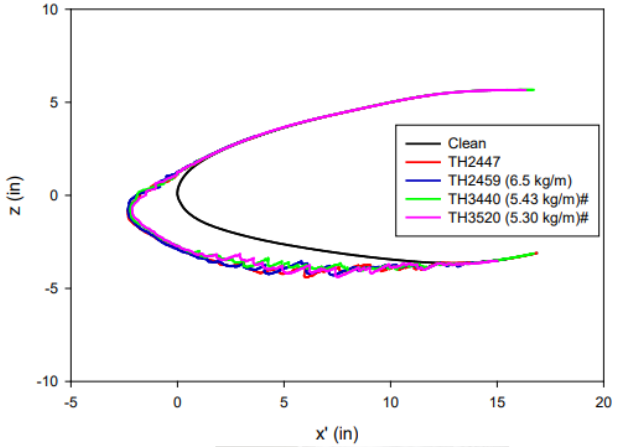

Case 1.3

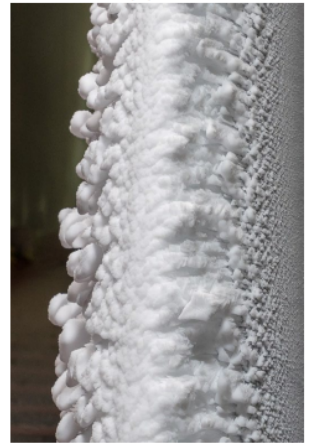

References: *Broeren et al., "*Ice-Accretion Test Results for Three Large-Scale Swept-Wing Models in the NASA Icing Research Tunnel", AIAA Aviation Forum, AIAA 2016-3733
Fujiwara, Bragg, Broeren, "Comparison of Computational and Experimental Ice Accretions of Large Swept Wings", J of A, Vol 57, No 2, 2020

Cases 2.1-2.3: CRM65 Inboard

IPW-2 Case no	AoA (deg.)	Flap angle (deg.)	Speed (knots)	Speed (m/s)	T_{total} (°C)	T_{static} (°C)	P_{total} (kPa)	P_{static} (kPa)	MVD (μm)	LWC (g/m^3)	Time (min.)	Freezing fraction	2015 ice mass (kg/m)
2.1	3.7	13.8	130	66.9	-1.4	-3.6	99.3	96.5	25	1.0	29.0	0.12	4.92
2.2	3.7	13.8	130	66.9	-6.3	-8.5	100.7	97.8	25	1.0	29.0	0.35	8.22
2.3	3.7	13.8	130	66.9	-23.8	-26.0	99.3	96.3	25	1.0	29.0	1.00	7.90

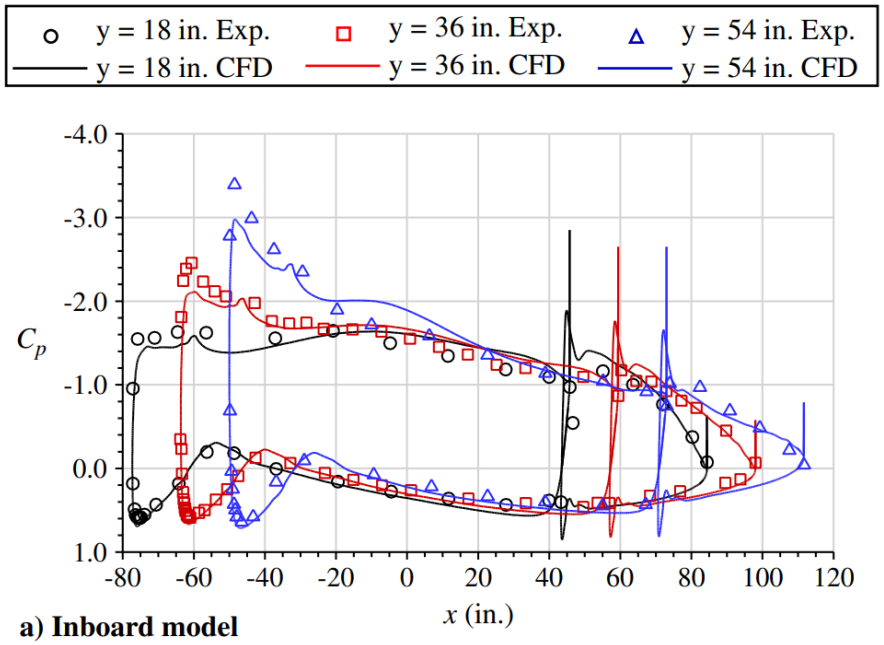

a) Inboard model

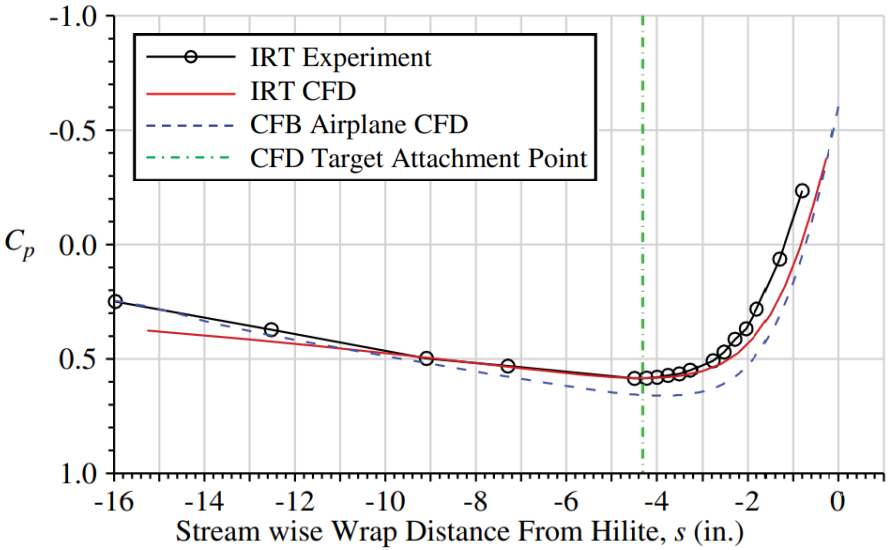

a) Inboard model

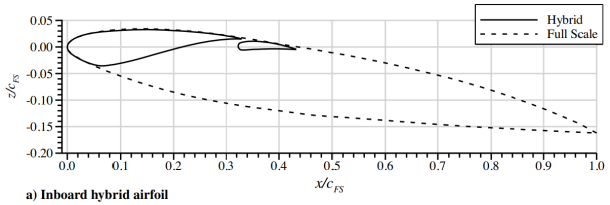

a) Inboard hybrid airfoil

- Workshop CADs provided at α = 0°, with the flap deflection built-in
- Grids are built after rotating the main element & flap assembly by +3.7° in Y axis about 0, 0, 0
- Pressure coefficients are based on inlet static pressure and density: CFD results that set back pressure at tunnel exit should use converged inlet static pressure as reference when computing C_P .

References: *Broeren et al., "*Ice-Accretion Test Results for Three Large-Scale Swept-Wing Models in the NASA Icing Research Tunnel", AIAA Aviation Forum, AIAA 2016-3733
Fujiwara, Bragg, Broeren, "Comparison of Computational and Experimental Ice Accretions of Large Swept Wings", J of A, Vol 57, No 2, 2020

Cases 2.1-2.3: CRM65 Inboard: Comparison of MCCS

IPW-2 Case no	AoA (deg.)	Flap angle (deg.)	Speed (knots)	Speed (m/s)	T_{total} (°C)	T_{static} (°C)	P_{total} (kPa)	P_{static} (kPa)	MVD (μm)	LWC (g/m^3)	Time (min.)	Freezing fraction	2015 ice mass (kg/m)
2.1	3.7	13.8	130	66.9	-1.4	-3.6	99.3	96.5	25	1.0	29.0	0.12	4.92
2.2	3.7	13.8	130	66.9	-6.3	-8.5	100.7	97.8	25	1.0	29.0	0.35	8.22
2.3	3.7	13.8	130	66.9	-23.8	-26.0	99.3	96.3	25	1.0	29.0	1.00	7.90

Test Condition 2

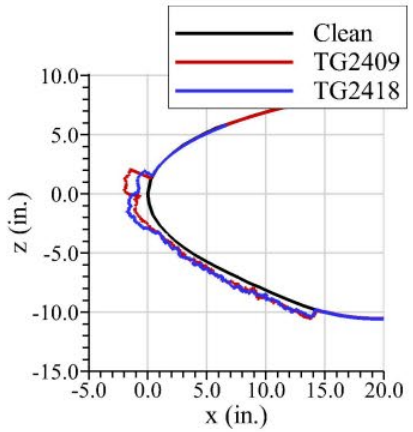

Test Condition 4

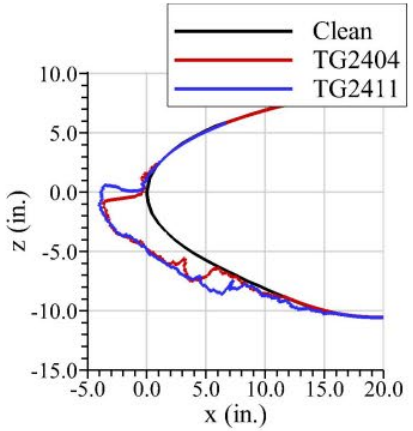

Test Condition 8

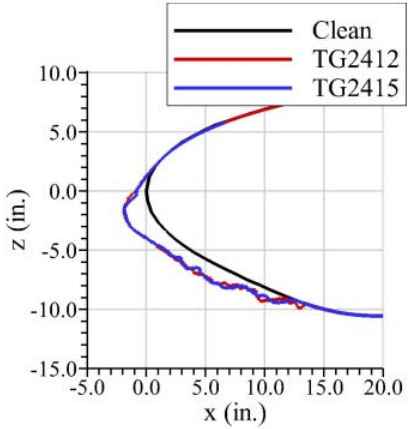

Case 2.1

Case 2.2

Case 2.3

References: *Broeren et al., "*Ice-Accretion Test Results for Three Large-Scale Swept-Wing Models in the NASA Icing Research Tunnel", AIAA Aviation Forum, AIAA 2016-3733
Fujiwara, Bragg, Broeren, "Comparison of Computational and Experimental Ice Accretions of Large Swept Wings", J of A, Vol 57, No 2, 2020

CRM65 Attachment Line Location

- Cases 1.1-1.3 Midspan Model
  - Suggest s = -1.49 inches ±0.25 in.
- Cases 2.1-2.3 Inboard Model
  - Suggest s = -4.49 inches ±0.25 in.

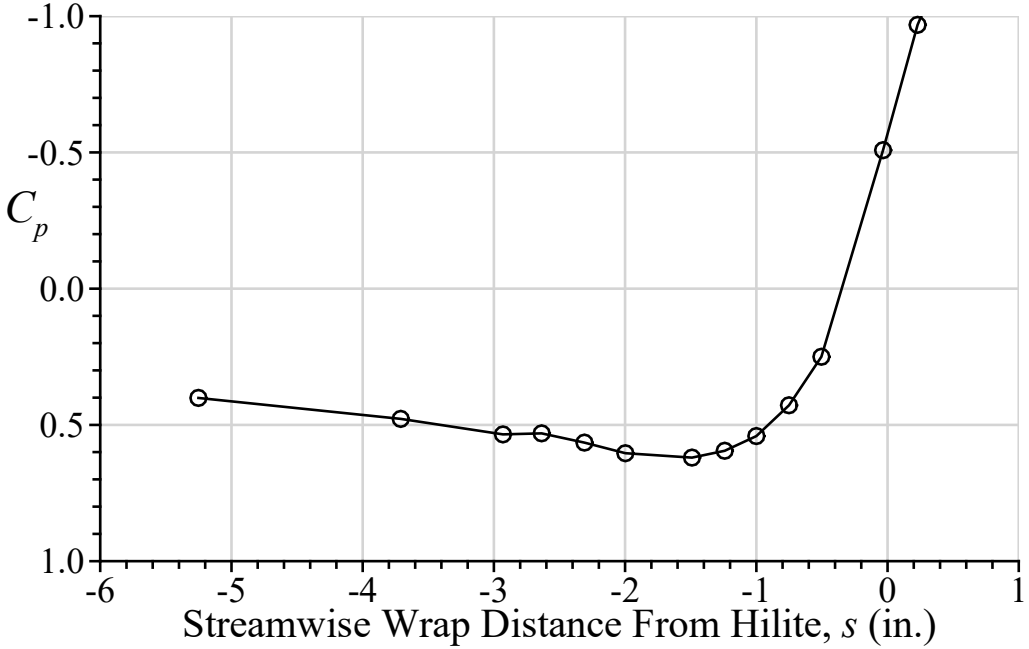

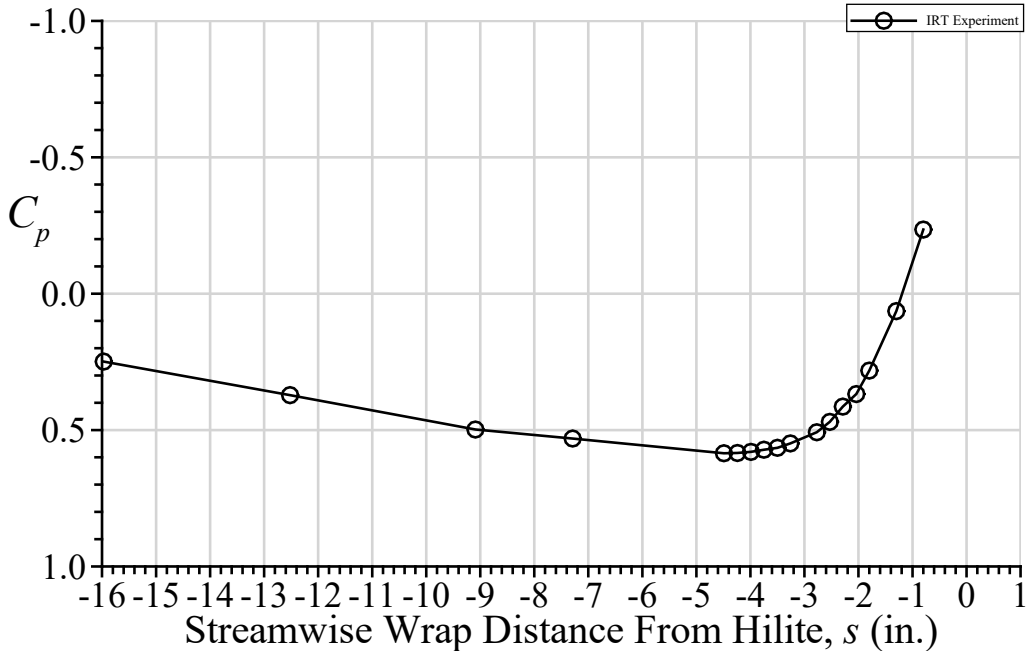

- Attachment line defined by location of maximum Cp.
- Location of hilite to be defined and provided.

NASA Glenn Research Center Icing Research Tunnel Cloud Calibration data

- This data is provided as recommendation for setting numerical simulation parameters
- Below is the cloud uniformity map for MVD = 20 µm and V = 150 knots take from NASA TM 2015-218758. The contour levels are ice thickness on the grid normalized by the average of the center 12 locations. Note that the test section is 72-inches tall.
- Data for uniformity contour plot available in electronic form.

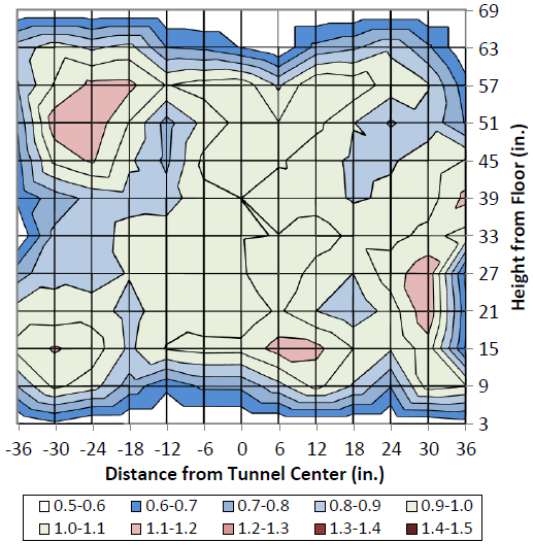

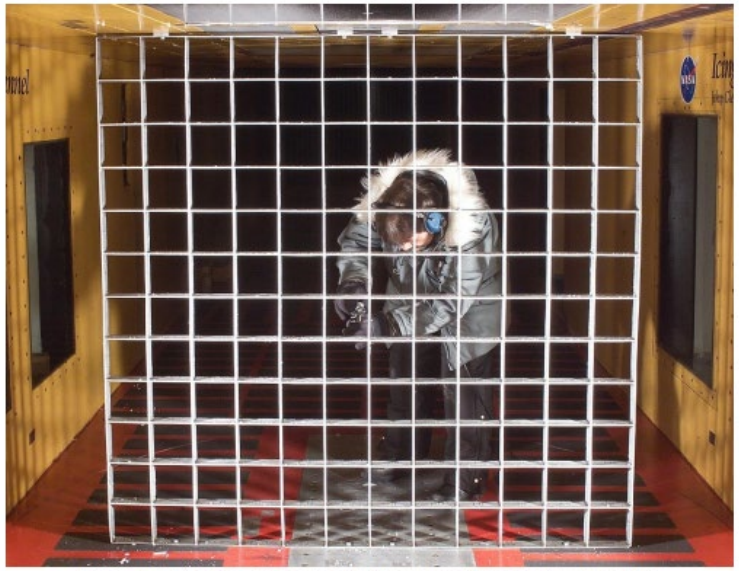

Figure 2.—A technician measures the thickness of ice accreted on the Grid.

- IRT distribution is different than Langmuir-D, and will be provided on the next page.

NASA Glenn Research Center Icing Research Tunnel Droplet Distribution

- The IRT distribution MVD = 24.9 µm is considered to be equivalent to the MVD = 25 µm provided in the conditions tables.

Drop Size [microns]	LWC [%]
7.3	5
9.9	10
13.7	20
24.9	30
44.9	20
74.9	10
127.6	5

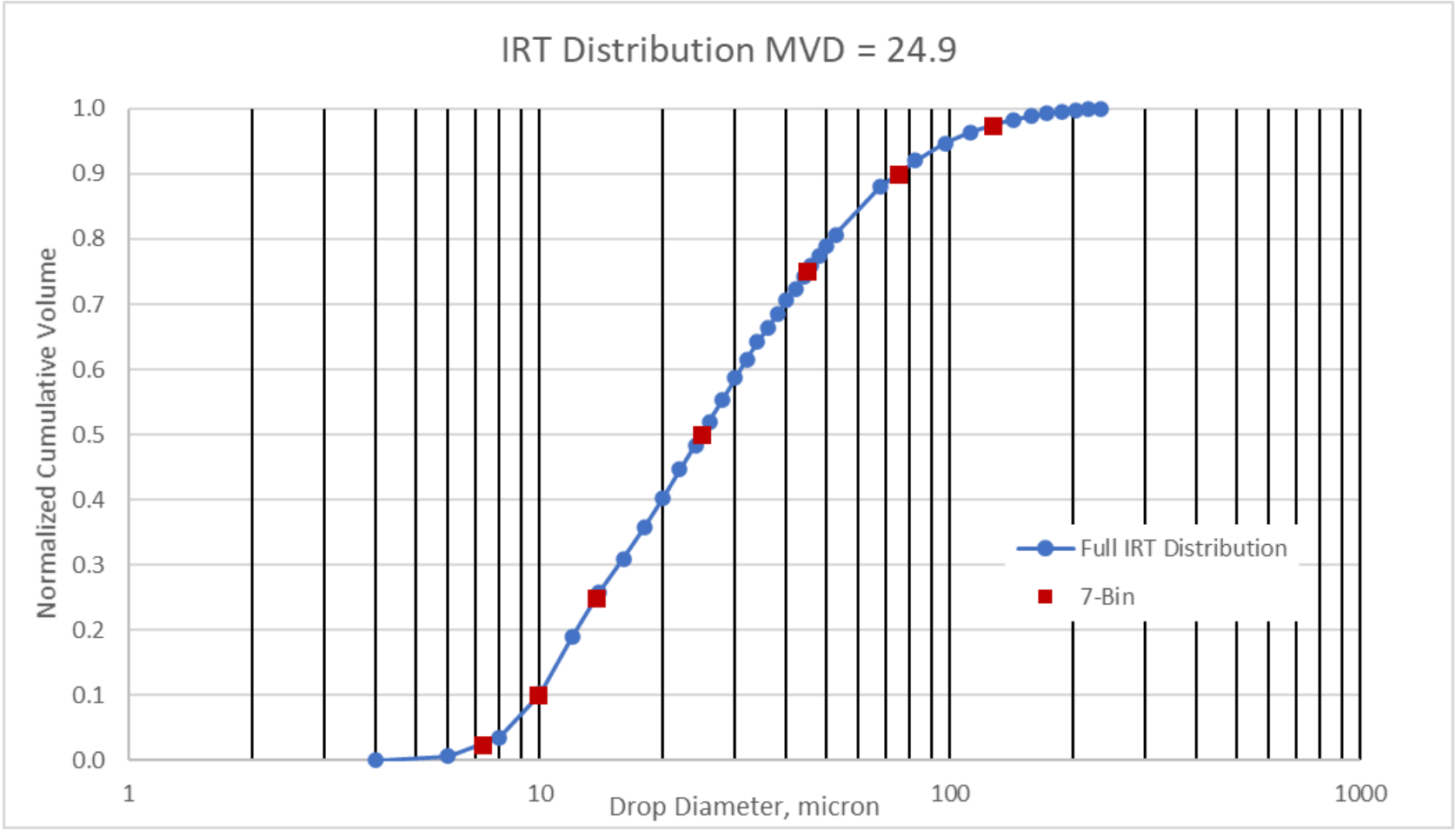

Additional Information for Cases 1 and 2

Location of static pressure used to calculate the experimental Cp

- Average value of two static pressures, P1 and P2 (x, y, z location measured from model center of rotation (CFD origin)).
  - P1 taken at x = -138.25 inches; y = 45.5 inches; z = -45.75 inches
  - P2 taken at x = -133.75 inches; y = 45.5 inches; z = 45.5 inches

Experimental Uncertainty in Tunnel Conditions

- From NASA TM 2015-218758
  - MVD uncertainty is ±10%
  - LWC uncertainty is ±10%
- From NASA CR-20210023627
  - Uncertainty in speed is ±0.9 knot
  - Uncertainty in test section static temperature is ±0.3 deg. C.
  - Uncertainty in test section total temperature is ±0.3 deg. C.
  - Uncertainty in test section static pressure is $\pm 5.5 \times 10^{-3}$ psi.
  - Uncertainty in test section total pressure is $\pm 5.7 \times 10^{-3}$ psi.

Effect of the ceiling gap in the CRM65 cases

- There is a 0.25 inch gap between the IRT ceiling and the CRM65 wing section models in the experimental setup
- Including this gap in the CFD analysis leads to more accurate aero results for the clean wing
  - Air flow through the gap reduces the wing/ceiling corner separation
  - The increase in separation size is quite large when the gap is closed, affecting Cp distributions and attachment line positions at y = 36 and 54 inch stations
- Icing tests and preliminary CFD icing analysis show that the pressure side of the gap closes with ice accretion
  - Photographs taken in the tunnel show ice at the ceiling/wing intersection, and some trace ice on the ceiling suction side away from the wing, following the boundary of the large vortex that forms at this junction
  - CFD results corroborate these findings, where simulations with FENSAP-ICE show complete blockage of the pressure side of the gap within 4 minutes of icing, and trace ice on the ceiling suction side
- Since the CFD meshes with the gap are more expensive and potentially difficult for multilayer icing codes to deal with, two versions are provided for the CRM65 cases:
  - Gap grids: tunnel floor and ceiling are built as viscous walls with a boundary layer grid, and the gap is resolved
  - No-gap grids: tunnel floor and ceiling are built as slip walls or symmetry boundaries without a boundary layer grid, and the gap is closed by extending the main element CAD

Effect of the ceiling gap in the CRM65 cases

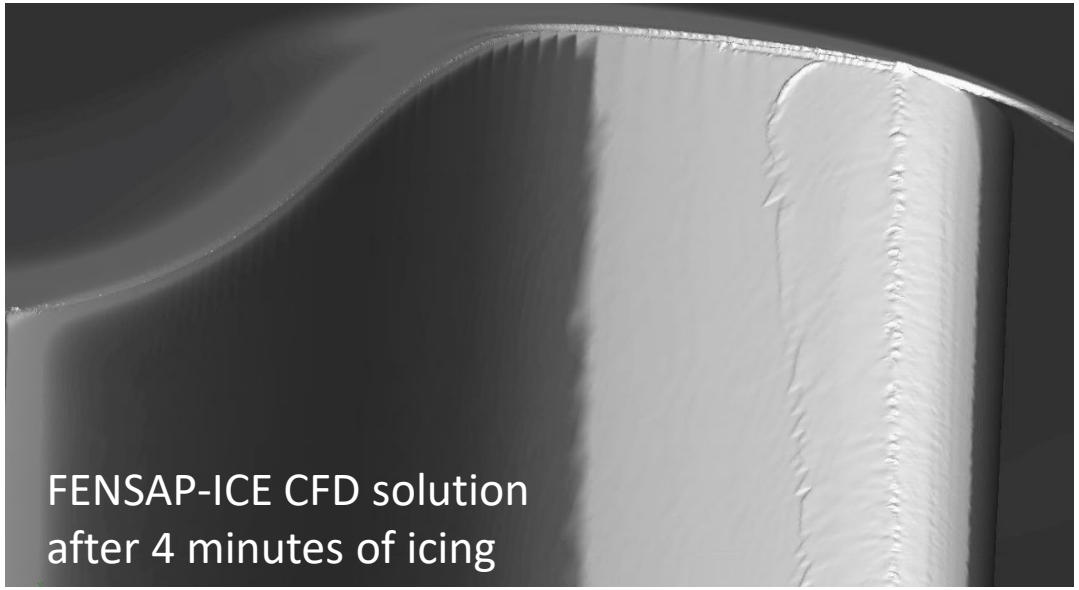

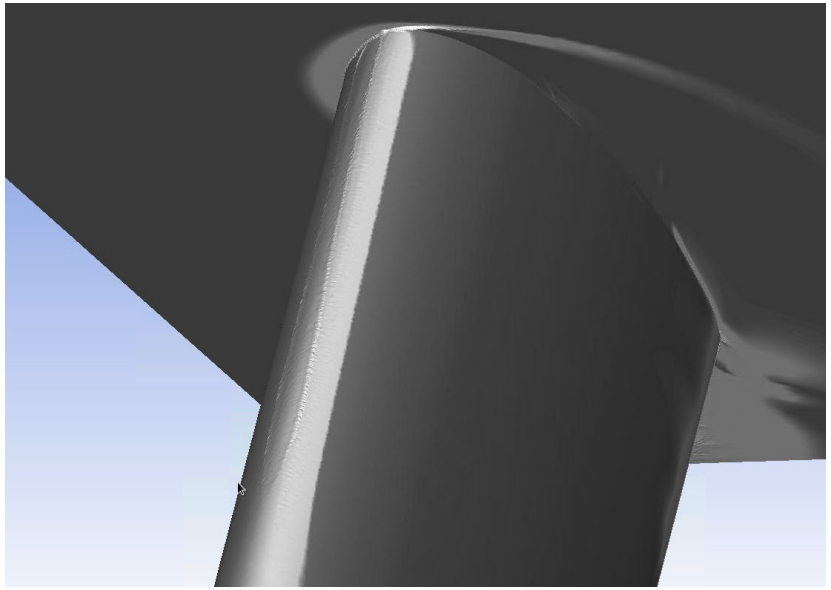

Top: Photograph showing ice blocking the gap in the experiment

Bottom: CFD icing solution showing gap closing within 4 minutes of icing

Effect of the ceiling gap in the CRM65 cases

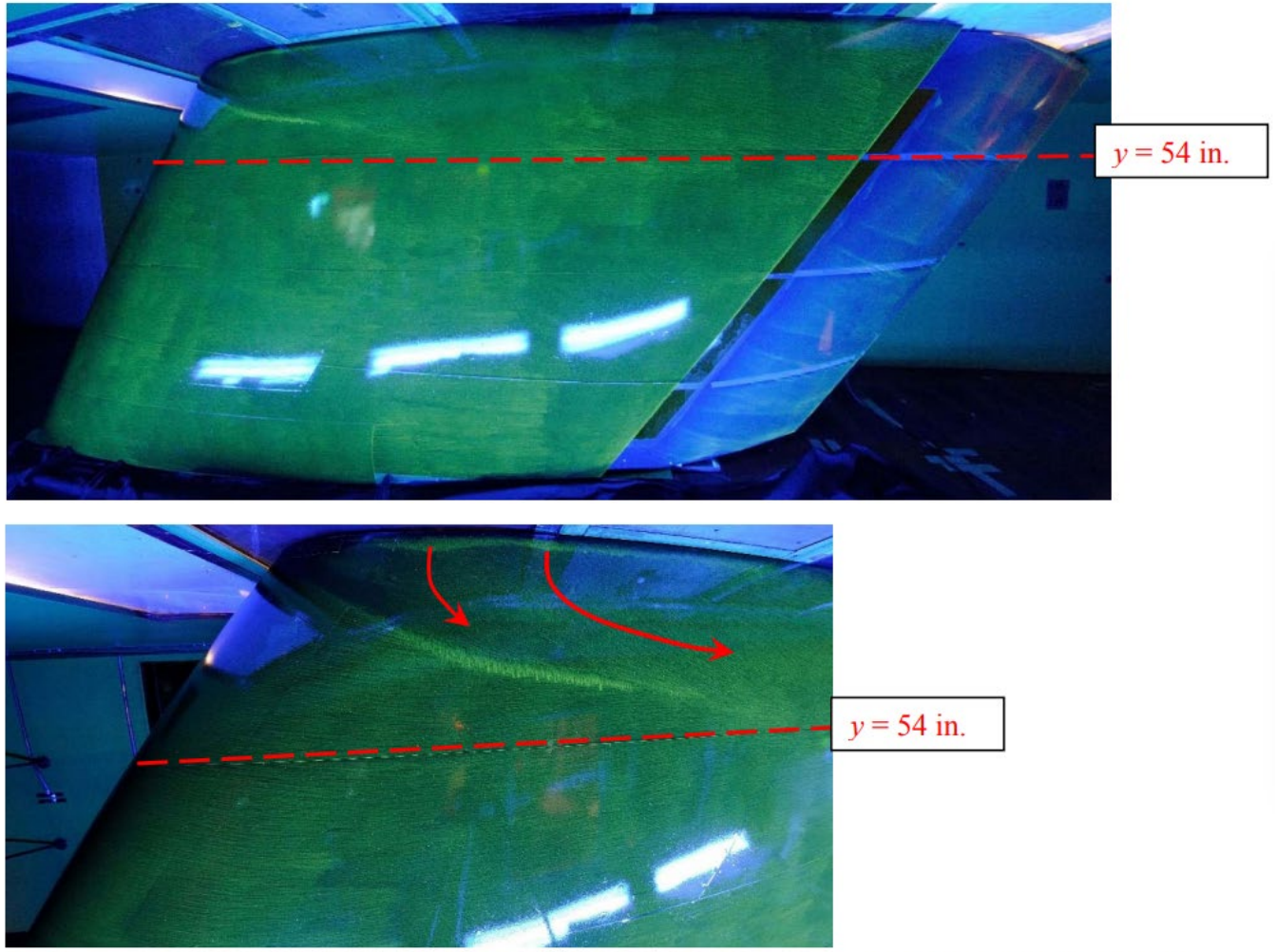

Figure 17. Surface oil flow visualization on Inboard model, α = 3.7 deg., Flap = 13.7 deg., 130 knots and total temperature = 12.0 ˚C.

Experimental evidence to flow separation at wing/ceiling junction

Figure from AIAA 2016 3733:

Ice-Accretion Test Results for Three Large-Scale Swept-Wing Models in the NASA Icing Research Tunnel

Andy P. Broeren[1] and Mark G. Potapczuk[2]
NASA John H. Glenn Research Center, Cleveland, Ohio 44135 USA

Sam Lee[3]
Vantage Partners, LLC, Cleveland, Ohio 44135 USA

Adam M. Malone[4] and Bernard P. Paul, Jr.[5]
Boeing Commercial Airplanes, Seattle, Washington 98124 USA

and

Brian S. Woodard[6]
University of Illinois at Urbana-Champaign, Urbana, Illinois 61801 USA

Effect of the ceiling gap in the CRM65 cases

CFD results with FENSAP and Fluent solvers showing surface shear stress magnitude

Using Spalart-Allmaras standard model, the separation with “no-gap” setup is quite large

Fluent with the kw-BSL (baseline) model produces a more realistic separation compared to the kw-SST model. SST encourages separation by design, and it can be tuned towards the BSL model by increasing the value of the “a1” constant

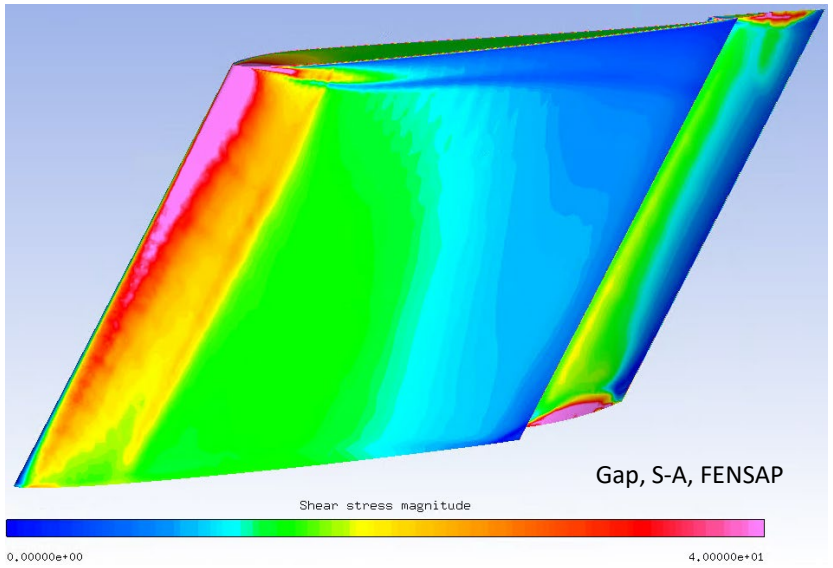

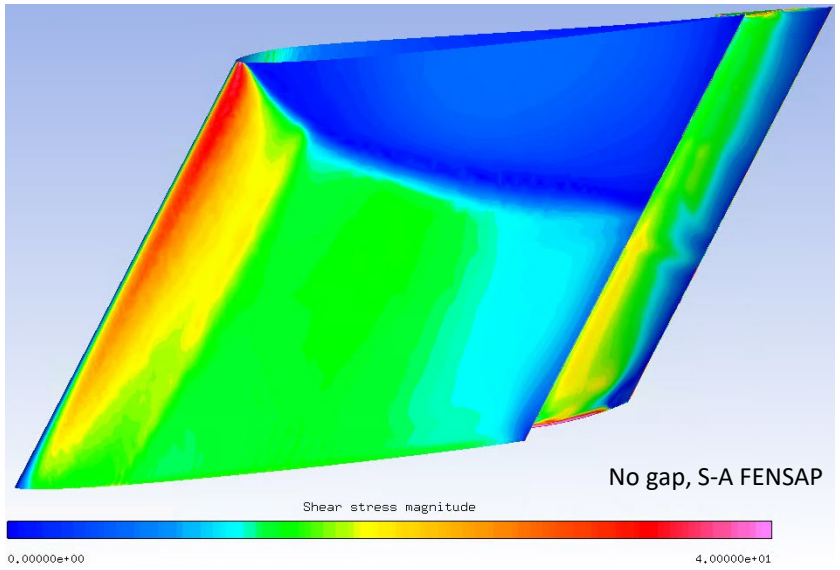

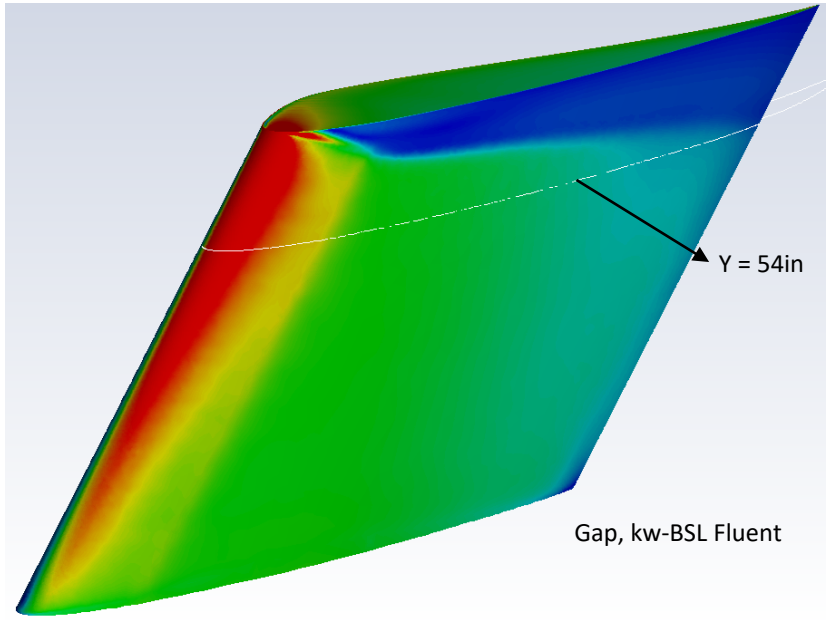

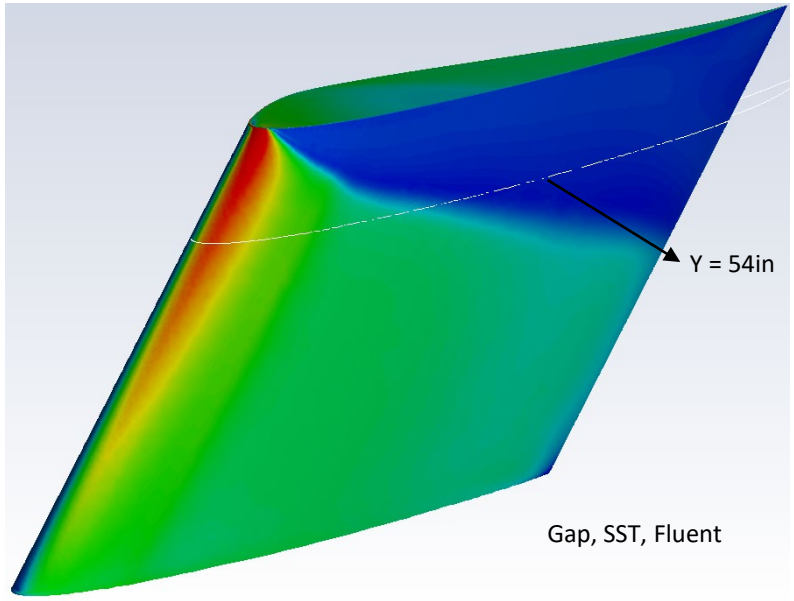

Effect of the ceiling gap in the CRM65 cases

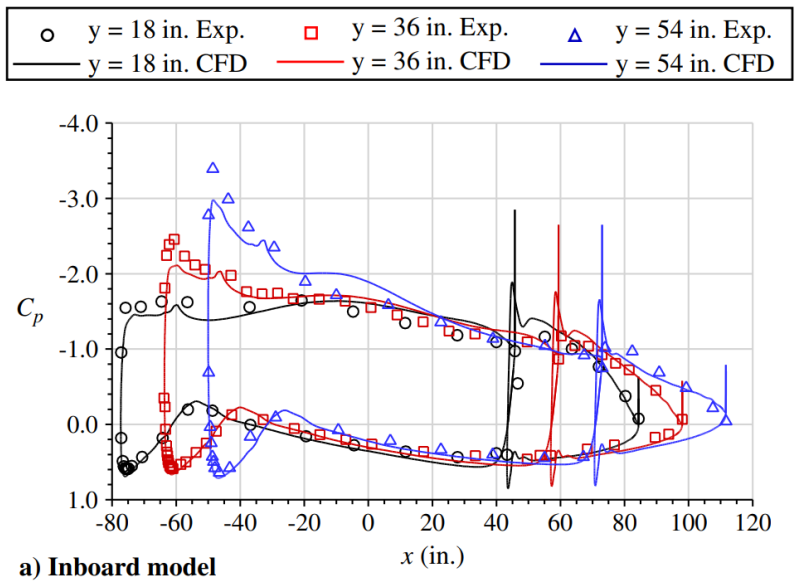

Exp & CFD from AIAA 2016-3733

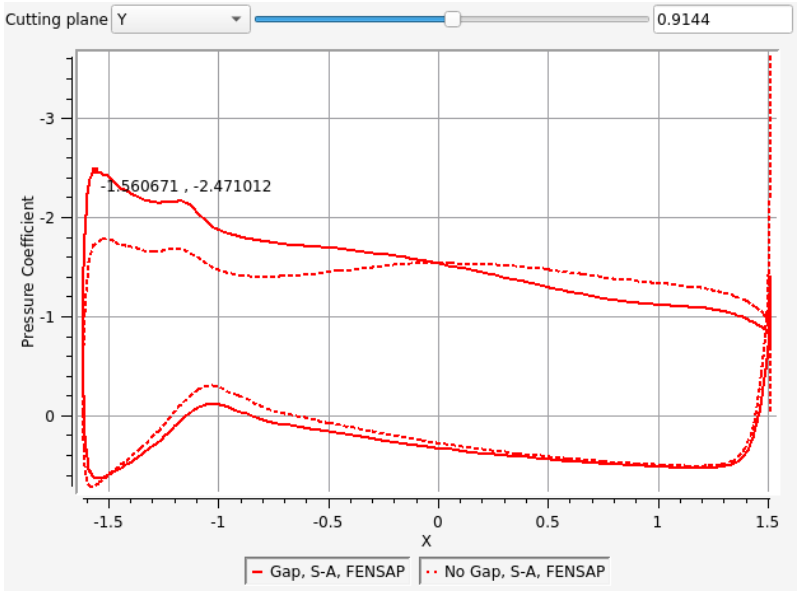

CFD: FENSAP S-A, gap vs no-gap at y = 36in, dimensions: tunnel coordinate system in meters

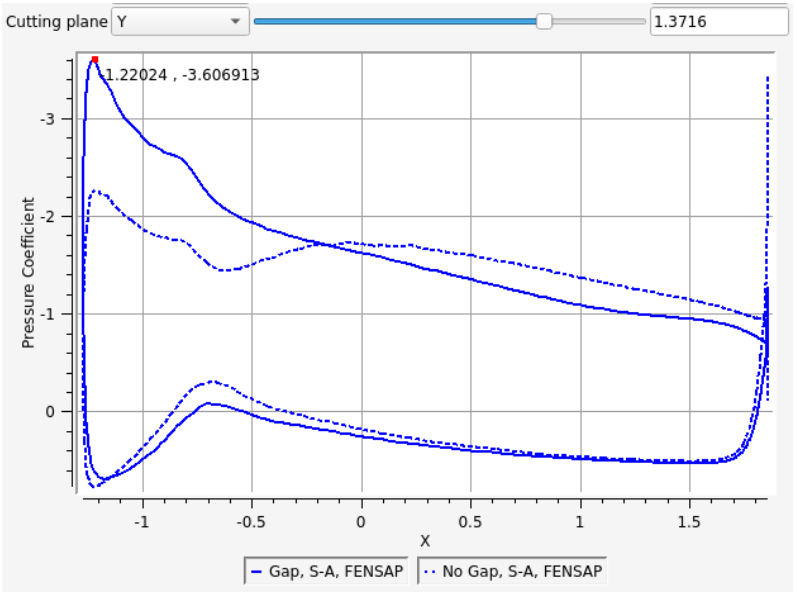

CFD: FENSAP S-A, gap vs no-gap at y = 54in, dimensions: tunnel coordinate system in meters

Pressure coefficient distributions at y = 36in and 54in stations are strongly affected by the size of the separation

Results where the gap flow resolved are more representative of the experimental measurements

Effect of the ceiling gap in the CRM65 cases

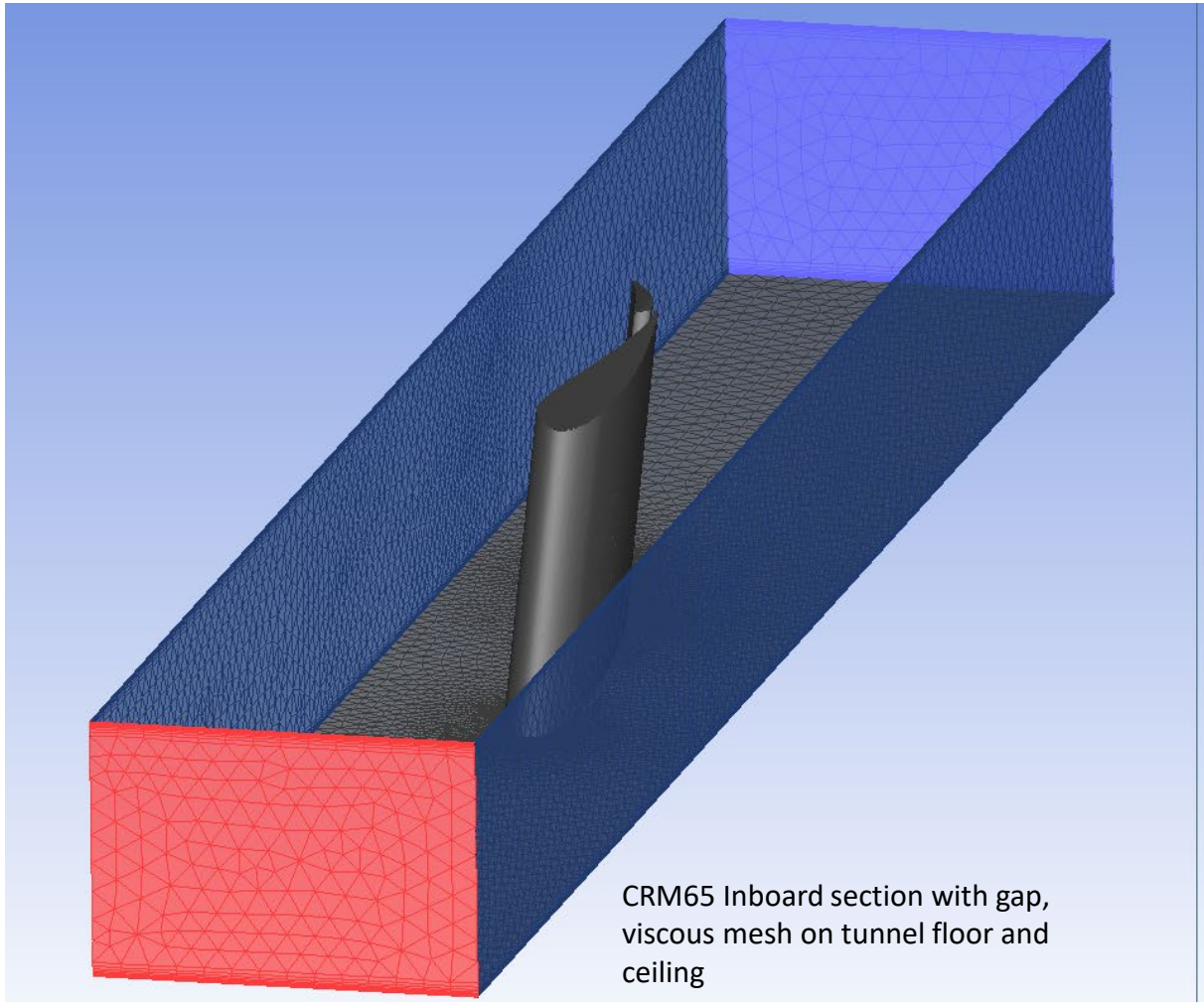

CRM65 Inboard section with gap, viscous mesh on tunnel floor and ceiling

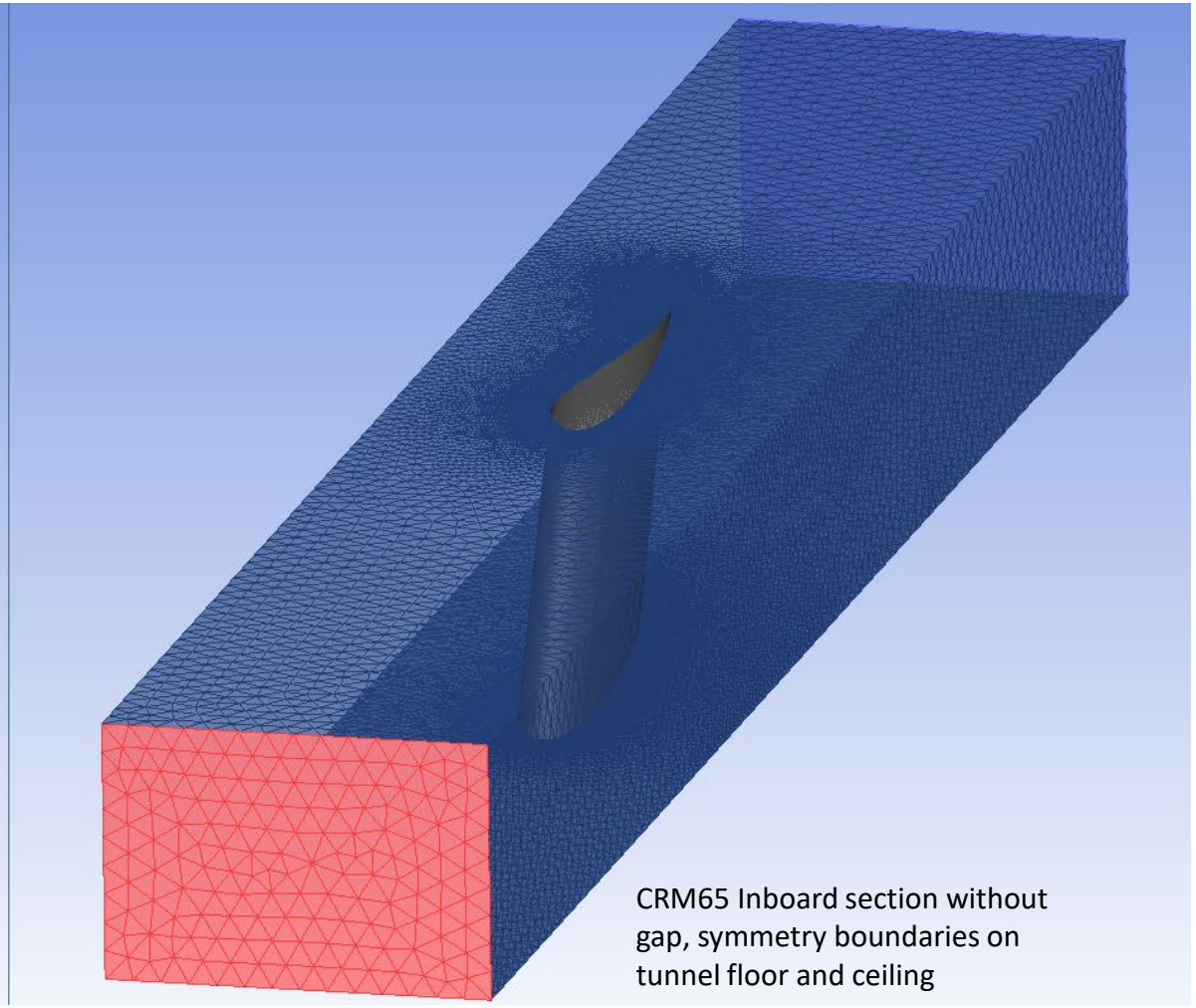

CRM65 Inboard section without gap, symmetry boundaries on tunnel floor and ceiling

Both grids with gap and no-gap setups are provided as part of the workshop grids

Cases 3.1-3.3: RG-15 Small Wing Low Speed Icing

IPW-2 Case no.	AoA (deg.)	Speed (m/s)	T_{static} (°C)	T_{total} (°C)	P_{static} (kPa)	MVD (µm)	LWC (g/m^3)	Time (min.)
3.1	4	25	-2.0	-1.7	101.3	24	0.44	20
3.2	4	25	-4.0	-3.7	101.3	24	0.44	20
3.3	4	25	-10.0	-9.7	101.3	24	0.44	20

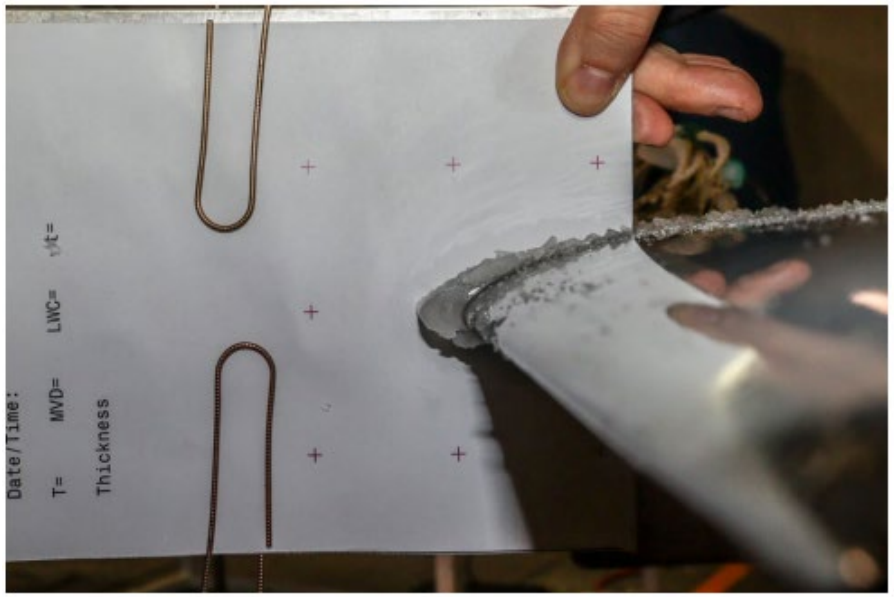

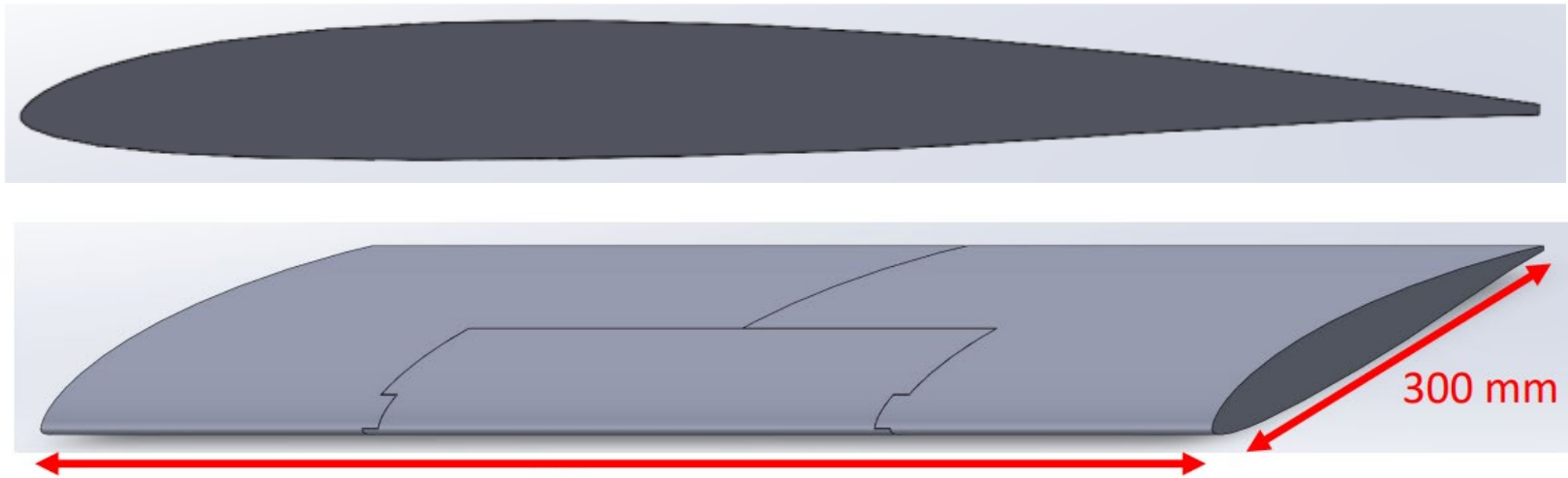

Reference: *NTNU UAV Icing Lab*

Cases 3.1-3.3: RG-15 Small Wing Low Speed Icing

Airfoil	RG-15
Span	0.58 m
Chord	0.30 m
Airspeed	25 m/s
Angle of attack	4 °
Liquid water content (LWC)	0.52 g/m³ *
Mean volume diameter (MVD)	27 microns *
Duration	20 min
Static temperature (glaze, mixed, rime)	[−2, −4, −10] °C
Reynolds numbers	$[5.7, 5.8, 6.0]\times10^5$
Relative Humidity	95–100%
Pressure	101.3 kPa

*Note, these values were updated after IPW2.

Publication: Hann, R., Müller, N.C., Lindner, M., Wallisch, J. (2023). UAV Icing: Experimental validation data for predicting ice shapes at low Reynolds numbers. SAE International Conference on Icing of Aircraft, Engines, and Structures. doi.org/10.4271/2023-01-1372

Droplet distribution for the low-speed icing cases (RG-15).

- Single bin MVD=27 µm is equivalent to the measured MVD=26.8 ± 1.5 µm.

Droplet Size [µm]	LWC [%]
7.3	5
12.5	10
18.7	20
26.8	30
36.8	20
51.2	10
81.3	5

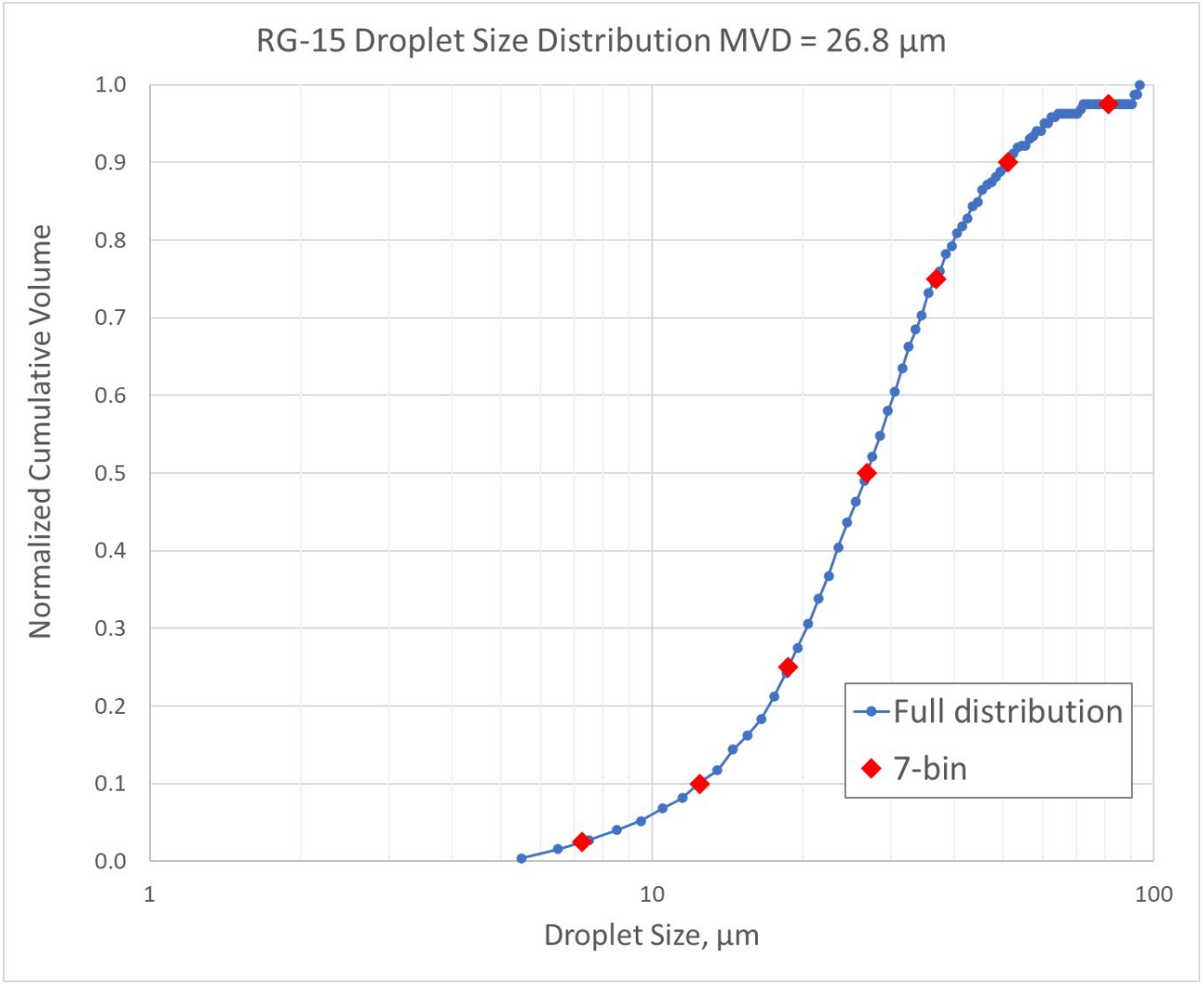

Icing wind tunnel setup

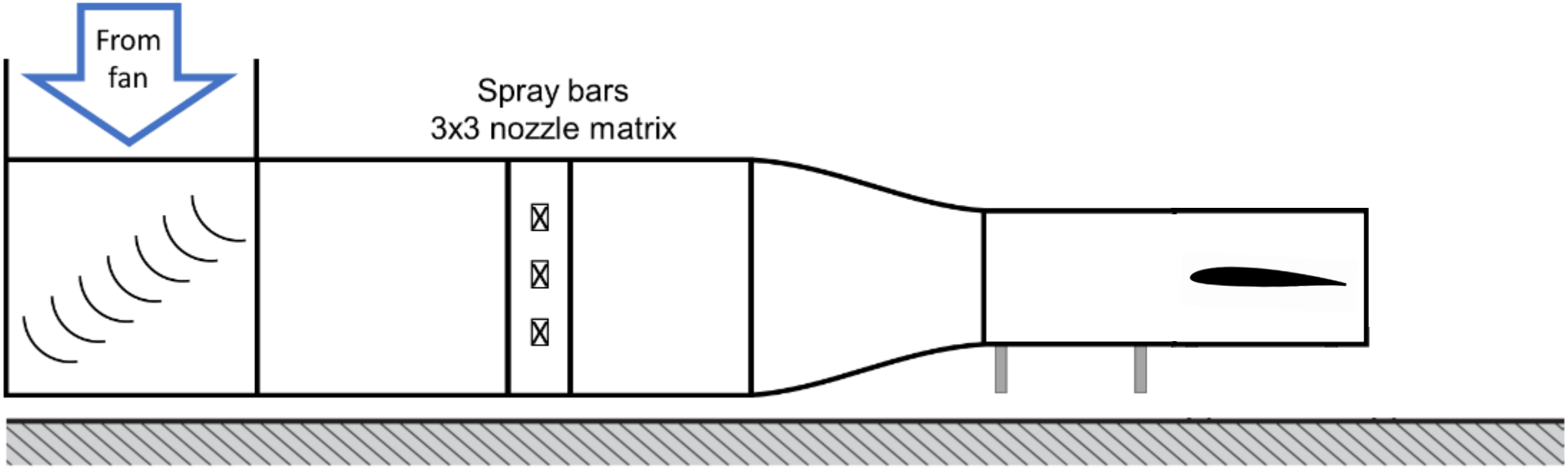

Cases 3.1-3.3: RG-15 Small Wing Low Speed Icing

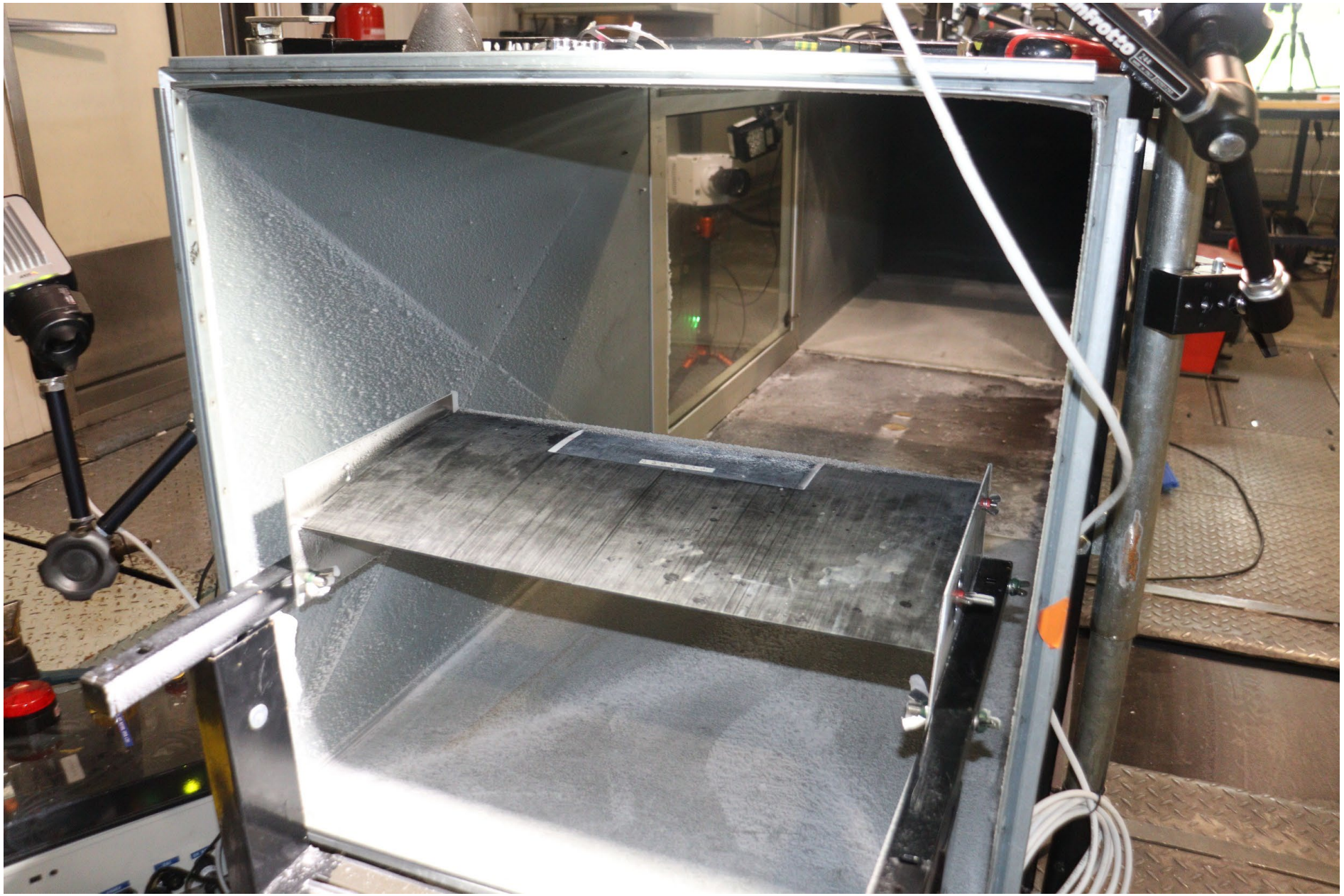

Cases 3.1-3.3: RG-15 Small Wing Low Speed Icing

Tunnel cross-section

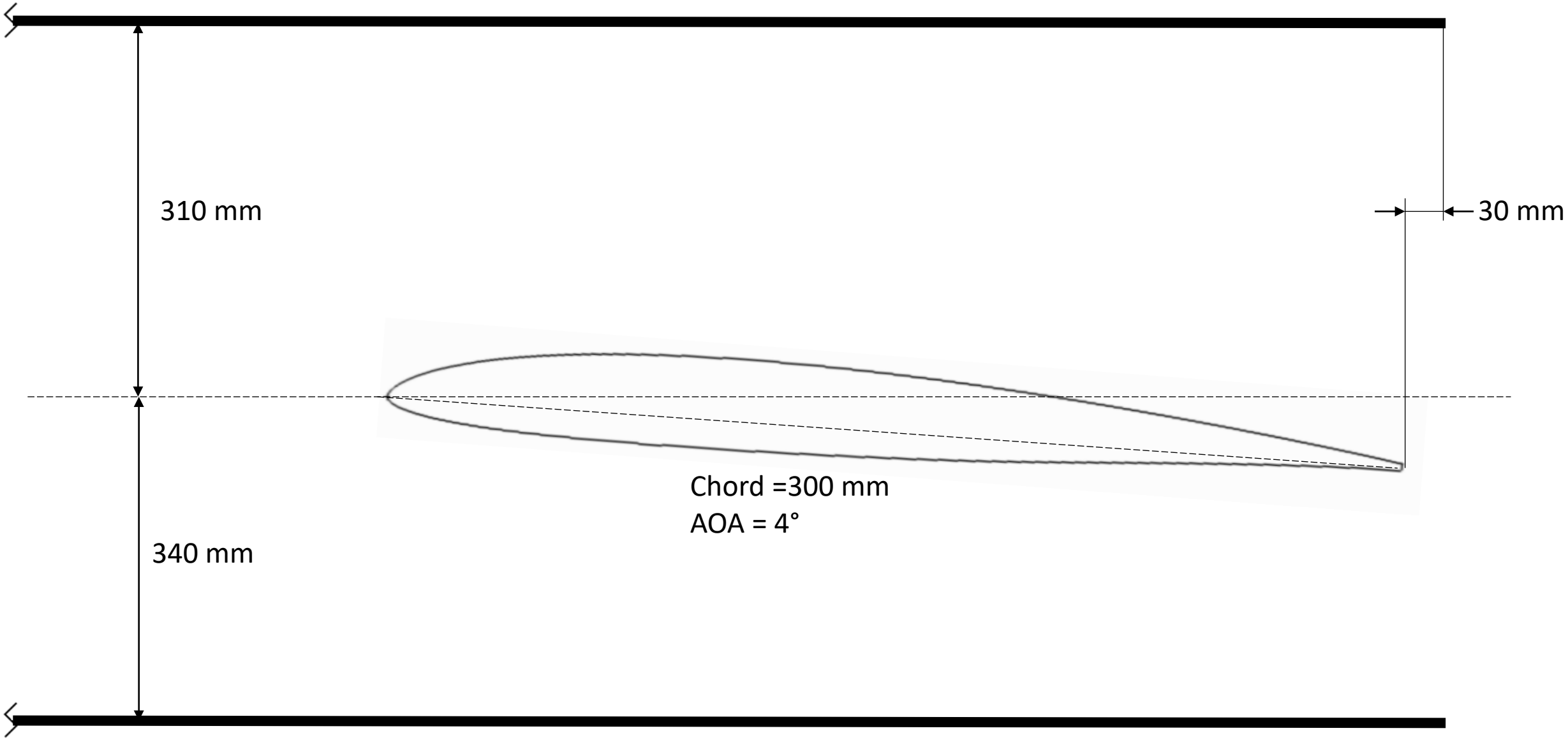

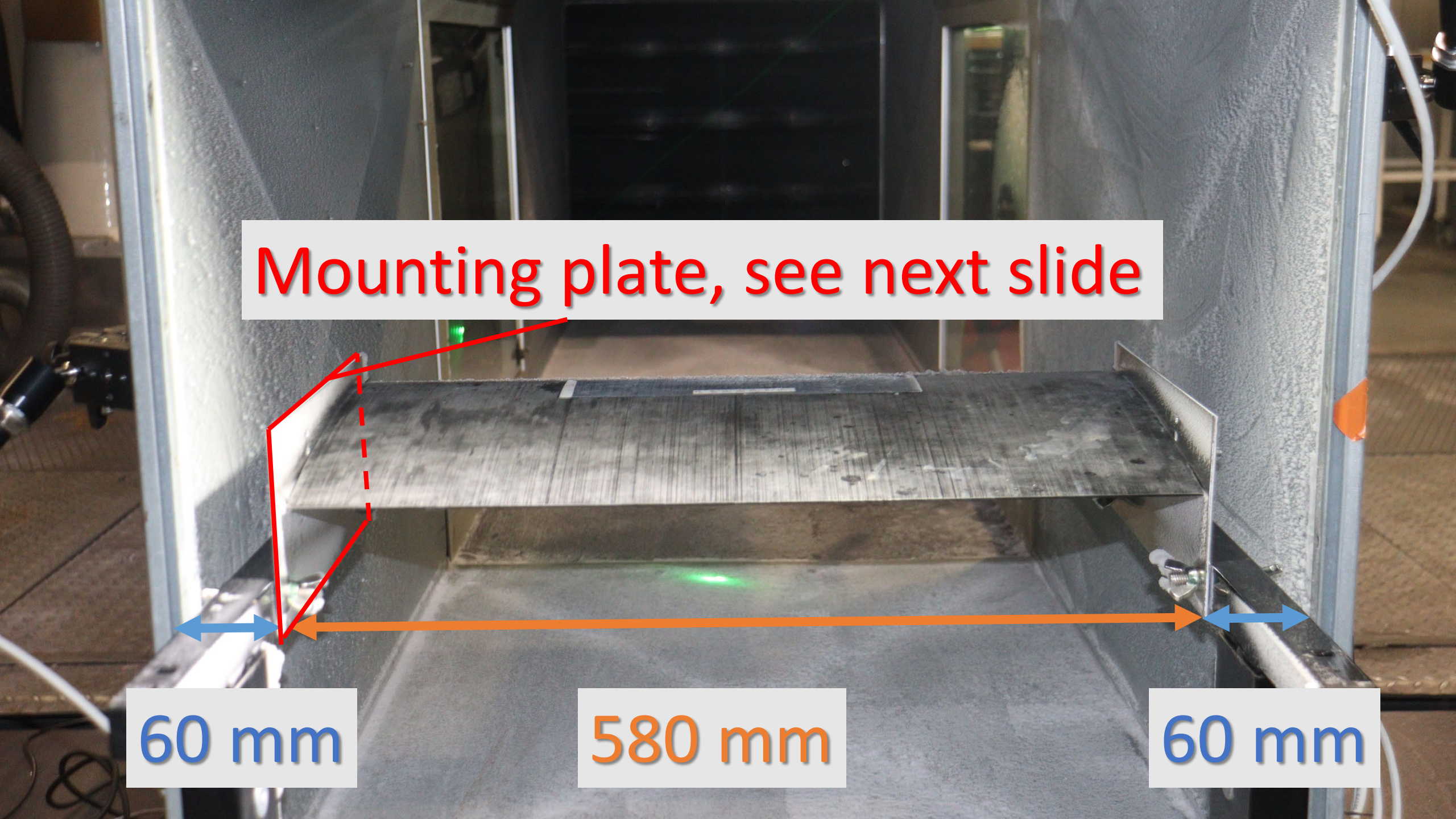
Mounting plate, see next slide
60 mm
580 mm
60 mm

Mounting plates

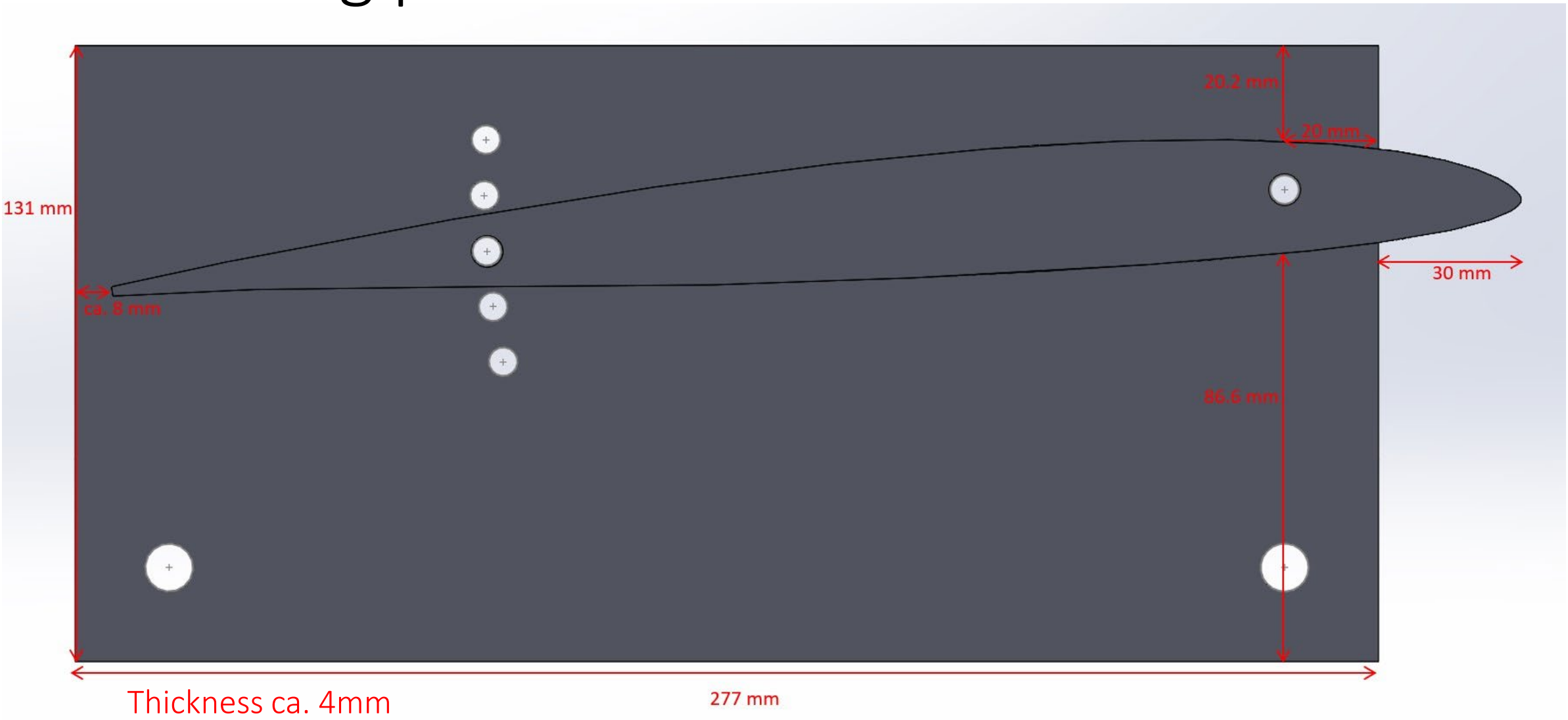

References

- Broeren, A., Potapczuk, M., Lee, S., Malone, A., Paul, B., Woodard, B. “Ice-Accretion Test Results for Three Large-Scale Swept-Wing Models in the NASA Icing Research Tunnel”, AIAA-2016-3733, doi: 10.2514/6.2016-3733
- Yadlin, Y., Monnig, J., Malone, A., Paul, B., “Icing Simulation Research Supporting the Ice-Accretion Testing of Large-Scale Swept-Wing Models”, NASA/CR—2018-219781
- Fujiwara, G., Bragg, M., Broeren, A., “Comparison of Computational and Experimental Ice Accretions of Large Swept Wings”, Journal of Aircraft Vol. 57, No. 2, March–April 2020
- Steen, L., Ide, R., Zante, J., Acosta, W., “NASA Glenn Icing Research Tunnel: 2014 and 2015 Cloud Calibration Procedures and Results”, NASA/TM—2015-218758
- Broeren, A., Lee, S., Bragg, M., Woodard, B., Radenac, E., Moens, F., “Experimental and Computational Icing Simulation for Large Swept Wings”, NASA/TP-20210023843
- Hann, R., Müller, M., Lindner, M., Wallisch, J., UAV Icing: “Experimental validation data for predicting ice shapes at low Reynolds numbers”, Technical Paper, International Conference on Icing of Aircraft, Engines, and Structures, accepted manuscript, 2023.